19th Brazilian Congress of Thermal Sciences and Engineering
November 6th–10th, 2022, Bento Gonçalves - RS - Brazil

# ENC-2022-0675
# AN EMPIRICAL ASSESSMENT OF ROLL WAVES EVOLUTION IN MUD-LIKE FLUIDS FLOWING DOWN STEEP SLOPES

**Valdirene da Rosa Rocho**
**Guilherme Henrique Fiorot**
**Sergio Viçosa Möller**
**João Batista Pereira**
**Evandro Fernandes da Cunha**
**Geraldo de Freitas Maciel**
valdirenerocho@gmail.com
guilherme.fiorot@ufrgs.br
svmoller@ufrgs.br
joao.pereira@unesp.br
evandrofernandesc@gmail.com
geraldo.f.maciel@unesp.br
Mechanical Engineering Graduate Program, Mechanical Engineering Department, Federal University of Rio Grande do Sul.
São Paulo State University, Ilha Solteira, SP.

***Abstract.*** *Free-surface flows are recurrent phenomenon observed in natural and industrial settings. They occur in inclined channels by the effect of gravity. The behavior of these flows is conditioned to the appearance of hydrodynamic instabilities, when present sufficient conditions for development and stabilization, we have what is known as roll waves. The study of these waves aims to examine necessary conditions to that the instabilities develop in time and space. This paper presents an experimental work that was carried out to observe and quantify certain aspects of the development of these waves in a laminar free-surface flow of non-Newtonian fluid of the Herschel-Bulkley type in many scenarios. The variation of the free surface interface was measured using an ultrasonic system. To study the problem, firstly it was identified the steady and uniform flow regime. Then, a disturbance with a fixed frequency was applied upstream of the channel, using a wave generator. It was observed that the stabilized waves present themselves as long waves and that the spatial evolution of roll waves follows an asymptotic behavior as a function of the distance traveled, presenting stabilization after traveling a few wavelengths. Also, it was noted that the amplitude of these waves depends on the Froude number and that the higher the Froude number, the higher the roll wave amplitude will be.*

***Keywords:*** *free-surface flow, non-Newtonian flow, Herschel-Bulkley, roll waves.*

## 1. INTRODUCTION

Recently several natural disasters have been happening in Brazil, and these have directly affected the environment and the Brazilian population in many states. Extreme events and natural disasters have been occurring worldwide as a direct result of climate change and human actions. In Brazil, in recent years, they have affected many regions, causing socio-economic damage and almost always taking lives (Maciel *et al.*, 2021). EM-DAT shows the trend of increasing natural disaster in Brazil (see Fig. 1), according to recent reports Brazil suffered, between 2012 and mid-2022, 58 natural disasters, which affected 44 million people and resulted in 1.405 deaths, and estimated damages of 13 million (EM-DAT, 2022).

Within this context, mud runs have been the object of many studies, for example, because they move large volumes and reach great distances. These phenomena are more frequent in valley areas with steep slopes (Balmforth and Liu, 2004; D'Alessio and Pascal, 2008).

The behavior of these shear flows is subject to several conditions, principles, and laws and also comes from problems related to them (Aktershev and Alekseenko, 2013; Needham and Merkin, 1984; Noble, 2007). Flows such as these,

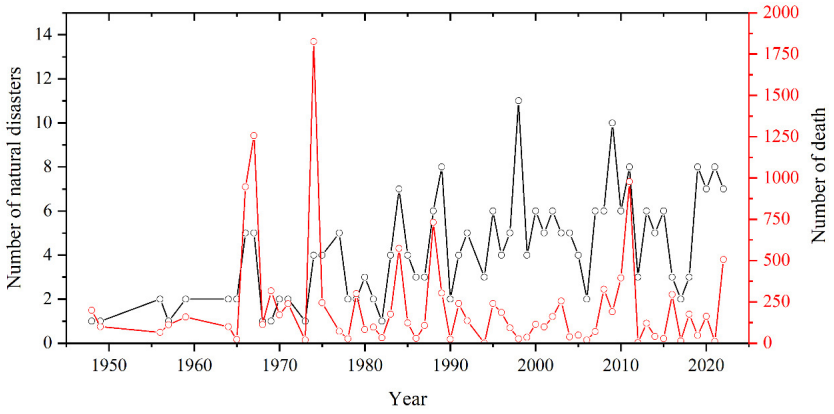


Figure 1: The number of natural disasters and deaths from these events in Brazil in the period from 1948 to 2022. Source: CRED, EM-DAT. The emergency events database, in: Cent. Res. Epidemiol. Disasters, 2022. https://www.emdat.be. Accessed in: 03th Jun 2022).

arising from natural disasters have been observed and recorded as they are subject to free surface instabilities (Maciel *et al.*, 2017). These instabilities when they develop and evolve into a stable pattern, and exhibit well-defined length, amplitude, and celerity are known in the literature as roll waves.

Roll waves arise in the vicinity of the uniform regime established by the flow, in an attempt to balance the inertial forces of the fluid, due to the action of the weight force (body force), with the viscous and frictional forces, which arise contrary to the flow. Furthermore, these instabilities only arise in the flow if geometrically and dynamically favorable conditions (Fiorot, 2012; Di Cristo *et al.*, 2013; Maciel *et al.*, 2017) exist, and furthermore if the disturbance imposed on it is within the specific frequency domain (Ferreira, 2013; Ferreira *et al.*, 2021).

Cunha (2018) highlights that in the experimental field, the pioneering work was that of Brock (1969), which provided a large amount of information about the formation of roll waves instabilities in turbulent flows of Newtonian fluid. The experiments of Brock (1969) were performed in a channel whose dimensions were: 0.11 m wide and 40 m long, with the slope varying between 5 and 10%. The depths of the flows in uniform regime were between 5 and 8 millimeters, with Froude numbers between 3 and 6.

In Newtonian fluids (e.g., water and glycerin) roll waves propagate with relatively high velocities when compared to non-Newtonian fluids (mud), under the same experimental conditions of flow rate and slope. In non-Newtonian fluids, roll waves present in avalanches, debris flows, mudflows, etc. tend to have longer wavelengths and amplitudes, which can potentiate the damage caused to property and infrastructure, even in the number of victims (Maciel *et al.*, 2017; Cunha, 2018).

Within this context, when it comes to physical experiments with roll wave development in the laboratory, some researchers choose to perform them in the laboratory by means of an experimental apparatus capable of reproducing and visualizing the signal of these waves Coussot (1994); Balmforth *et al.* (2005); Fiorot *et al.* (2015); Maciel *et al.* (2017), among others.

Fiorot *et al.* (2015) and Maciel *et al.* (2017) have invested their efforts in the development and operationalization of an experimental apparatus capable of generating and accurately measuring roll waves in highly viscous, Newtonian (glycerin), and non-Newtonian rheology fluids (Carbopol gel). Gel as a substitute fluid presents the advantage of being transparent facilitating the visualization technique when it does not present rheometric properties similar to the muds in dam foot and races (Cunha, 2018).

For the development of this work give to continued the works of the Rheology of Viscous and Viscoplastic Materials Research Group (RMVP Group), which focused on the study of roll waves from experiments performed in the form of Herschel-Bulkley-type fluid flows in different scenarios, under slopes ranging from 13º to 20º. The experiments were performed in a rectangular channel, 3.00 m long and 0.30 m wide, and discharge rates of 0.88 to 1.07 $l/s$.

Thus, this study aimed to perform experimental tests with test fluid Carbopol gel in the channel. The manufactured gel presents a Herschel-Bulkley rheological behavior, is transparent, provides good visualization of free surface phenomena, and was produced only for this purpose; to control the process of disturbance and measurement of the roll wave phenomenon by means of ultrasonic sensors in order to obtain some of the characteristics of these waves after data processing. It is hoped that this communication will contribute to existing gaps in the literature on roll waves in non-Newtonian rheology.

## 2. MATERIALS AND METHODS

In order to evaluate the process of spatial stabilization of roll waves this study employed the experimental apparatus for generating, stabilizing, and measuring surface instabilities developed by Fiorot (2012); Fiorot *et al.* (2015); Maciel *et al.* (2017). The experiments consisted of imposing an air jet, with frequency and intensity controlled using an Arduino controller, on a test fluid flow (Carbopol 996 Gel). The measurements of the free surface and its oscillations were performed from ultrasonic transducers placed at different points along the channel.

### 2.1 Experimental apparatus

The experimental apparatus consists of equipment necessary to ensure controlled flow conditions, rheological characterization of the test fluid, and measurement of roll waves with precision. Thus, the apparatus is composed of several modules, in which each one plays a recurring role, configured by a specific and dedicated work methodology for each function performed (Cunha, 2018). The roll wave generation and measurement apparatus is constituted of different systems, which include the test fluid circulation, generation, and measurement of surface instabilities. Figure 2 illustrates the operating flowchart of the roll wave generation and measurement apparatus.

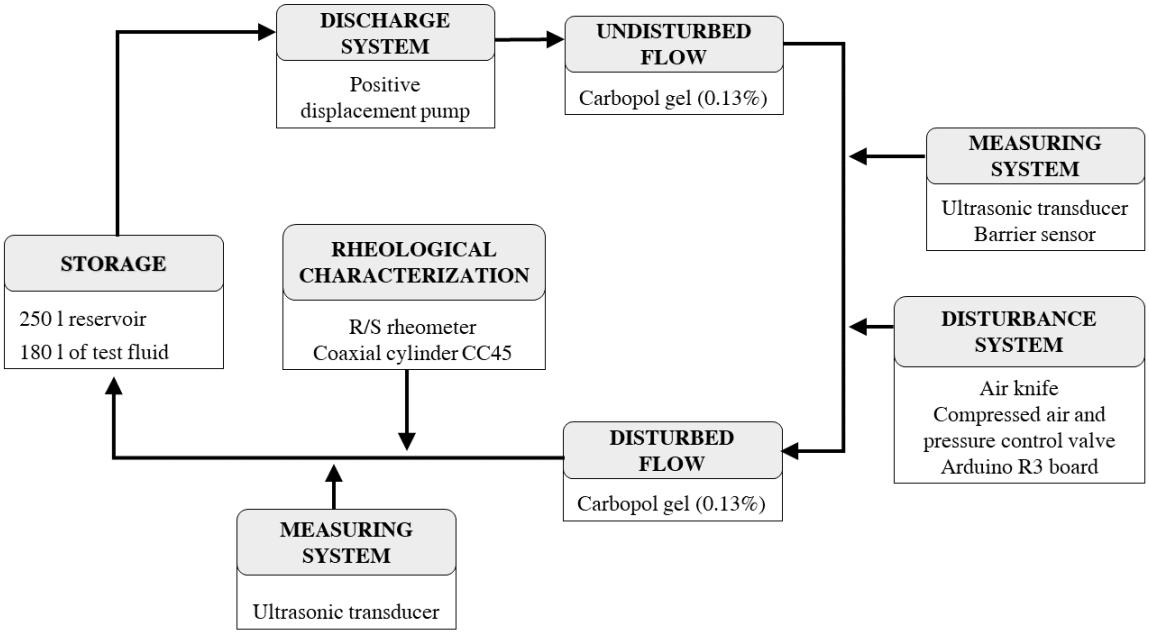


Figure 2: Operational diagram of the operation of the pulsed wave generation apparatus.

Figure 3 presents the details of the experimental apparatus, in a plan drawing, positioning each module that makes up the experimental apparatus in the same position as the operating scheme, as represented by the flowchart described in Fig. 2.

Figure 3: Experimental apparatus in isometric view (Cunha, 2018).

### 2.1.1 Fluid circulation and pumping system

The flow took place in an inclined channel (of variable inclination) of 3 meters long and 30 centimeters wide through the use of a progressive cavity hydraulic pump (rotating positive displacement and indicated for viscous fluids) with a rotation controller. The pumping and circulation system proved to be adequate, especially for generating low agitation of the fluid and also for the low levels of noise transferred to the flow. In order to avoid the generation of bubbles in the flow, a PVC device was built and attached at the end of the channel, which allowed the smooth transfer of the fluid between the channel and the reservoir.

### 2.1.2 Flow height measurement system

To measure the height of the flow and surface instabilities, ultrasonic transducers based on the pulse-echo technique were used, thus ensuring no interaction between the measurement system and the generated phenomenon. Three RPS-401A transducers were used, which were incorporated into the measurement chain after their calibration curves were obtained. The calibration curves of the transducers were obtained from the correlation between electrical voltage and distance measurements performed on a micrometer.

The measurement interface of the ultrasonic transducers was implemented in LabView software. A National Instruments acquisition board (Model USB-6009) was used to connect the software to the sensors. From the LabView software, it was possible to both visualize and acquire and store the data at the time of the experiments. The data acquisition rate was set at 100 Hz and this value was sufficient to obtain data without overlapping effects when analyzing the spectra in the frequency domain.

### 2.1.3 Disturbance system

The perturbation system employed in this research consists of a perturbation system consisting of an air knife (produced from additive manufacturing) with an opening of 1 mm width and a length of 30 cm coupled to a pressure valve fed by an air compressor. The air pulse generation, with defined power and frequency, was controlled by an Arduino board. The disturbance frequency used in all experiments was 1.5 Hz.

### 2.1.4 Rheological characterization of the fluid

The experiments were performed with Carbopol gel, a viscoplastic fluid, produced from the polymer Carbopol 996, with rheological characteristics similar to the materials found in natural flows (Piau, 2007). The carbopol gel was produced in the mass concentration of 0.13% and in the quantity of 180 liters, according to the methodology defined by Minussi and Maciel (2012).

Currently, there are several devices capable of measuring such properties. The simplest ones provide only the viscosity, while the most sophisticated ones, in addition to the flow curve, allow the adjustment of a good rheological model for the fluid under analysis.

The flow curve of the test fluid was obtained from a rheometer (Brookfield R/S, strain rate, and shear stress control) with the coaxial system and spindle CC-45. The procedure consisted in imposing two stages of strain rate: an ascending and a descending one; and the respective measurement of the shear stress, according to Fig. 4.

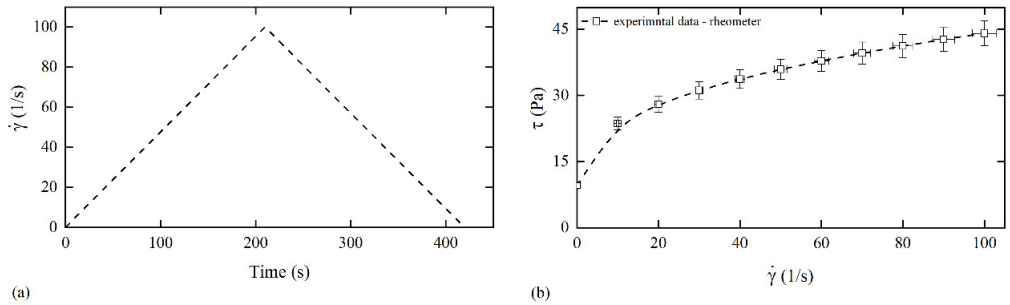


Figure 4: Rheological characterization: (a) characterization protocol and (b) flow curve obtained for the fifth test.

The analysis of the flow curve and obtaining the $\tau$ = shear stress, as well as the parameters: $\tau_0$ =yield stress, $k_n$ =consistency index of the fluid and $n$ =flow index, which was done according to the use of the Herschel-Bulkley model, according to Eq. (1), considering the ascending branch of the flow curve and strain rate in the range $1 < \dot{\gamma} < 100\ ^1/_s$.

$$\tau = \tau_0 + k_n \dot{\gamma}^n \tag{1}$$

The results of the rheological characterization of the test fluid for each experiment, and in terms of the rheological parameters, in addition to the specific mass measurements, were performed from the calibrated volume and are presented in Tab. 1. According to Maciel *et al.* (2017) the Carpobol gel can be represented by the equation characterizing the Herschel-Bulkley rheological model.

### 2.2 Characterization of the flow regime

In this work, we search to determine some important dimensionless for the nature of the flows treated in this paper, among them, we obtained the critical stress, which is defined as a function of the characteristic parameters of the flow and the properties of the fluid, i.e., (Eq. 2):

$$C = \frac{\tau_0}{\rho g h_0 \sin(\theta)}. \tag{2}$$

To classify the hydraulic regime of the flow in the channel, it was sought to evaluate its motion by means of the dimensionless numbers R and F. The Reynolds number (R) is a dimensionless number that relates the inertial and viscous forces acting on the fluid in motion:

$$\mathsf{R} = \frac{2\rho u_0^2}{\tau_0 + k_n(2u_0/h_0)^n}. \tag{3}$$

The characterization of the flows in terms of free surface energy is measured by the Froude number (F), which is defined by the relationship between the inertial and gravitational forces:

$$\mathsf{F} = \frac{u_0}{\sqrt{g h_0 \cos\theta}}. \tag{4}$$

From these dimensionless, it is verified that the flow is laminar, the flow is considered to be of laminar type, where the fluid particles travel parallel trajectories. Where, $u_0$ is the average velocity of the flow, $g$ acceleration of gravity, $h_0$ depth of flow in uniform regime, $\theta$ the channel slope, $\rho$ the specific mass (Maciel *et al.*, 2017).

### 2.3 Experiments

Different materials and equipment were used to perform the roll waves stability experiments, as presented in section 2. The experiments were conducted according to different channel slopes (between 13 and 20°) and disturbance system with frequency of 1.5 Hz. A set of five flow rates were tested (between 0.88 and 1.07 $^{l}/_{s}$) and, for each fixed flow rate, a data set of the flow in uniform regime and with presence of roll waves was measured.

It was considered that the beginning of the experiment occurred after the flow reached the uniform regime, in this condition the following information was obtained: flow rate ($Q$) from the gravimetric method and mass flow determination - a total of 10 repetitions; depth of the uniform flow ($h_0$) by means of the ultrasonic transducers; mean flow velocity ($u_0$) according to the relation between flow rate (use of the gravimetric method) and flowing section; surface velocity ($u_s$) using barrier sensors installed in two sections of the channel - a total of 10 repetitions. Table 1 presents the results measured in the experiments and the physical and rheological properties of the test fluid. It is worth pointing out that these values are obtained from an average, since the records were taken several times until a good precision was obtained for the results.

Table 1: Fluid properties and experimental results.

| Test | $Q$ ($^{l}/_{s}$) | $\theta$ | $h_0$ (mm) | $u_0$ ($^{m}/_{s}$) | $u_s$ ($^{m}/_{s}$) | $\rho$ ($^{kg}/_{m^3}$) | $\tau_0$ (Pa) | $k_n$ (Pa.s$^n$) | $n$ | C | R | F |
|---|---|---|---|---|---|---|---|---|---|---|---|---|
| 1st | 1.01 | 13º | 13.73 | 0.25 | 0.33 | 1003.2 | 8.09 | 3.73 | 0.42 | 0.27 | 20 | 0.69 |
| 2st | 0.89 | 15º | 12.72 | 0.23 | 0.23 | 1000.9 | 8.08 | 3.98 | 0.29 | 0.25 | 17 | 0.67 |
| 3rd | 1.07 | 15º | 13.04 | 0.27 | 0.35 | 1003.4 | 7.52 | 4.50 | 0.40 | 0.23 | 22 | 0.78 |
| 4th | 0.88 | 20º | 12.15 | 0.24 | 0.32 | 1003.2 | 9.56 | 5.73 | 0.39 | 0.23 | 14 | 0.72 |
| 5th | 1.00 | 20º | 12.56 | 0.27 | 0.35 | 1003.2 | 9.56 | 5.73 | 0.39 | 0.23 | 17 | 0.78 |

Once the measurements of the uniform flow were performed, the disturbance system was triggered, and, according to the flow characteristics and slopes different characteristics of surface instabilities appeared. The surface instabilities were recorded from 3 ultrasonic transducers installed at different positions in the channel, namely: 0.3 m, 0.6 m, 0.9 m, 1.2 m, 1.5 m, 1.8 m, 2.1 m, and 2.4 m from the disturbance source. The transducers at positions 2.1 and 2.4 m were fixed, while the third transducer was moved between positions 0.3 and 1.5 m, as shown in Fig. 5(a). It was taken into account that for the generation of roll waves type instabilities the favorable domain condition, i.e., $\mathsf{F} > \mathsf{F}_{\min} \approx 0.23$ must be respected.

The uncertainties of the measurements obtained were calculated from the combined standard uncertainty, which used the standard uncertainty of the equipment used and the standard deviation, according to Eq. (5).

$$U = k\sqrt{U_A^2 + U_B^2}, \tag{5}$$

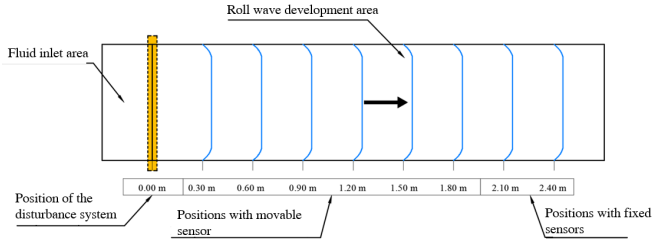


(a) Schematic of the positioning employed for the disturbance system and ultrasonic transducers.

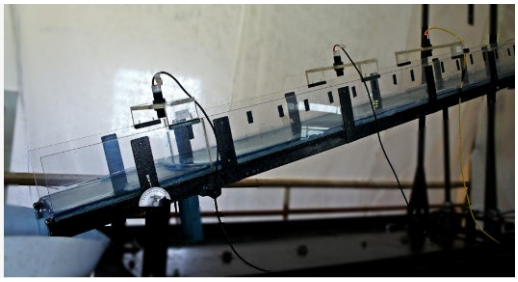

(b) Roll waves generated in an inclined channel.

Figure 5: Schematic of the channel and the roll waves generated from it.

where $U$ is the total uncertainty, $k$ is the Student's coefficient, $U_A$ is the uncertainty related to the accuracy of the equipment, and $U_B$ is the uncertainty due to the standard deviation.

To perform the flow measurement, the weighing procedure was adopted. For each fixed channel inclination, the frequency inverter was manipulated to make the pump perform a certain number of revolutions per minute. With the aid of a bucket and stopwatch, two members of the research group timed the time required to fill the bucket with an unknown volume of Carbopol gel flowing downstream from the canal. This volume was then weighed on a scale and noted down. This procedure was done ten times for each slope-flow binomial. The accuracy of each instrument used is listed below in Tab. 2.

Table 2: Accuracy of the equipment used.

| Instrument | Measured quantity | Precision (%) |
|---|---|---|
| Rheometer | Pa, Pa.s$^s$, s$^{-1}$ | $\pm$ 3.00 |
| Digital chronometer | s | $\pm$ 0.20 |
| Digital balance | mass (g) | $\pm$ 0.10 |
| Ultrasonic transducer | distance (mm) | $\pm$0.29 |

For the analyses performed in this work, a confidence interval of 95.5% and Student's coefficient were used according to the amount of sample employed for each experiment. Considering the precision of the equipment and the standard deviation of the experiments, the errors associated with the measured parameters were estimated as shown in Tab. 3.

Table 3: Uncertainties of the measured flow properties.

| Flow property | Measurement unit | Uncertainty (%) |
|---|---|---|
| Height of flow $(h)$ | mm | $\pm$ 0.70 |
| Volumetric flow rate $(Q)$ | $\mathrm{m^3/s}$ | $\pm$ 3.10 |
| Mass density $(\rho)$ | $\mathrm{kg/m^3}$ | $\pm$0.40 |
| Average velocity $(u_0)$ | $\mathrm{m/s}$ | $\pm$3.30 |
| Superficial velocity $(u_s)$ | $\mathrm{m/s}$ | $\pm$1.30 |
| Yield stress $(\tau_0)$ | Pa | $\pm$6.30 |
| Consistency rate of the Herschel-Bulkley fluid $(k_n)$ | Pa.s$^n$ | $\pm$6.30 |
| Flow index $(n)$ | – | $\pm$6.10 |

Note that in Tab. 3 all the uncertainties of the flow properties have been presented.

## 3. RESULTS

Within the experimental context, tests were performed with Carbopol gel for different channel slopes and volumetric flow rates. The purpose of such tests was to generate pulsating roll waves. These waves were generated under the imposition of a disturbance. Initially, the fluid was injected into the channel by means of a pump and allowed to flow for a certain time until the flowing fluid reached a uniform permanent regime.

In the sequence, a disturbance is applied on the free surface of the flow with a fixed frequency. Regarding the roll waves measurement, after the disturbed flow, they were recorded at eight different points in the channel, i.e., the sensors were installed according to the following distance: 0.3 m, 0.6 m, 0.9 m, 1.2 m, 1.5 m, 1.8 m, 2.1 m and 2.4 m from the disturbance source; the last one was located at 0.6 m from the channel exit. It is worth noting that there were only three

sensors installed in the channel, but one of them was moved according to the length specified above, in order to have resulted in eight different positions along the channel.

After gauging the wave (roll wave) by the ultrasonic and photometric measurement systems, the treatment of the data began by applying the equations resulting from the calibration curves, in order to transform the signal (electrical voltage), into the depth of flow in measurement units (millimeter). After this development, three more processes were necessary so that the data obtained could be compared and studied.

In Fig. 6 the profiles of the roll waves observed for one of the cases studied (fifth test) for the eight sensors are illustrated. It is possible to note the behavior of the wave along the channel, as well as its evolution until stabilization occurs.

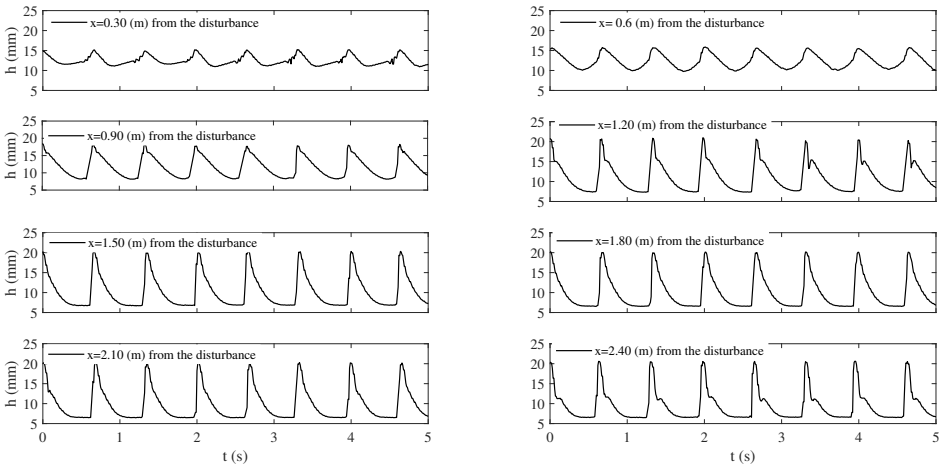


Figure 6: The evolution of the roll waves was recorded at eight different positions in the channel. Experimental results for the fifth test.

In Fig. 6 the illustration of the waves detected by the eight sensors is shown, and it was possible to observe the wave motion along the channel and its evolution until complete stabilization. Note that they present the characteristics of roll waves, that is, waves with steep fronts, well-defined wavelength, and amplitude, observations like these are also made by Fiorot *et al.* (2015). It is also possible to notice that at approximately $x = 1.2$ m the roll waves start to present similar height amplitude, i.e., their stabilization happens after traveling through $x = 1.2$ m of the channel. This process is repeated for another four tests and the respective waves and uniform regime are captured.

A quick observation of the result will allow the statement that the period of the waves, $T$, is identical to the period imposed on the channel disturbance. This observation can be concluded by taking the spectrum of the signal, as shown in Fig. 7.

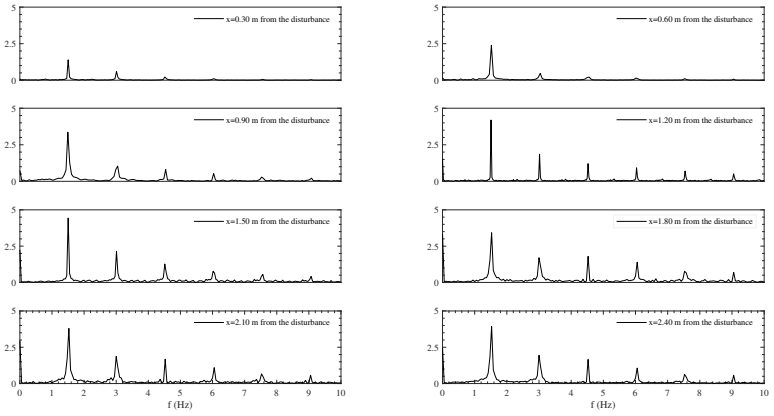


Figure 7: Spectral amplitude of the waves at different points in the channel.

Since it is a periodic signal in the time domain, the Fourier transform was used to identify the spectral density of the signal. From Fig. 7 it can be seen that the wave spectrum is similar in both cases, and there is a dominant frequency, i.e., the one with the highest power is 1.5 Hz. We see that the signal has most of its energy concentrated at the frequency imposed on the system. Also, it was noted that in all cases the period of the waves, $T = 0.66$ s.

It is worth noting that the other slopes and flow rates were tested: 1.01 $^{l}/_{s}$, 0.89 $^{l}/_{s}$, 1.07 $^{l}/_{s}$, and 0.88 $^{l}/_{s}$, and their results were the same. It can be seen that, in fact, the system is amplifying the imposed disturbance at the same frequency. It can be seen that the signal has most of its energy concentrated at the frequency imposed on the system.

In addition, the spectral analysis of signals with different amounts of measured waves indicated the need, when performing the physical experiment, to capture at least ten measured waves in order to preserve the behavior of the signal in the frequency domain.

Also, we sought to compare the roll wave profiles for two of the cases studied (2st and 5 th test ). These waves were monitored at the spatial position $x = 2.1$ m. This distance is related to the distance between the disturbance system and the sensor that registers the signal of the generated waves, see Fig. 8.

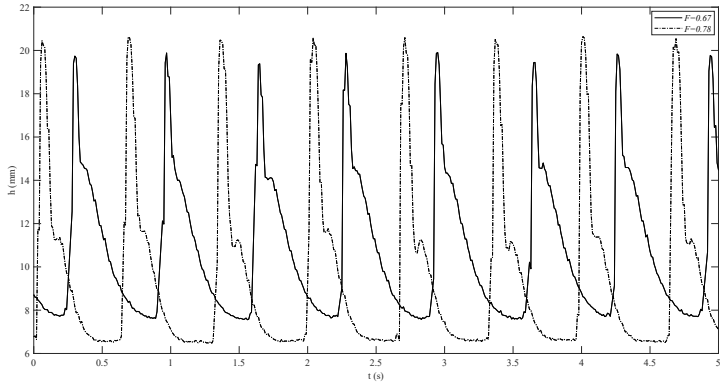


Figure 8: Comparison chart between the waves generated for each volumetric flow rate configuration ($\mathsf{F} = 0.67$ and $\mathsf{F} = 0.78$).

It can be seen in Fig. 8 that as the Froude number increases, the wave amplitude also increases, coming in agreement with the observations was also made by Fiorot *et al.* (2015); Maciel *et al.* (2017). Another important characteristic identified in roll waves is the propagation speed of these waves, also known as wave celerity $(U)$. This was obtained using the following equation (Eq. 6) (Ng and Mei, 1994; Fiorot *et al.*, 2015; Rocho *et al.*, 2020):

$$\frac{U}{u_0} = \alpha + \sqrt{\alpha^2 - \alpha + \frac{1}{Fr^2}} = \frac{\lambda}{T}, \tag{6}$$

where

$$\alpha = \left(\frac{2n+1}{3n+2}\right) \frac{2\left(n+1\right)^2 + n\left(4n+3\right)C}{\left(n+1\right)^2 + 2n\left(n+1\right)C + n^2C^2}. \tag{7}$$

is the vertical velocity distribution coefficient (Eq. 7), and it was determined from the rheological parameters of the fluid, using the literature of Maciel *et al.* (2013). Once the period of the wave was determined by analyzing the signal spectrum and the velocity $U$, it was possible to determine the wavelength ($\lambda$), see Tab. 4.

Table 4: Characteristic properties of the roll waves generated in the execution of the experiments.

| Test | $\Delta h$ (mm) | T (s) | U ($^{m}/_{s}$) | $\lambda$ (m) |
|---|---|---|---|---|
| 1st | 11.800 | 0.66 | 0.645 | 0.43 |
| 2st | 10.669 | 0.66 | 0.610 | 0.41 |
| 3rd | 11.387 | 0.66 | 0.663 | 0.44 |
| 4th | 12.523 | 0.66 | 0.604 | 0.40 |
| 5th | 13.736 | 0.66 | 0.639 | 0.43 |

In Tab. 4 the waves properties for each experimental test are presented, among them, we highlight the amplitude $(\Delta h)$, period $(T)$, propagation velocity $(U)$, and wavelength $(\lambda)$, both very well defined. Regarding the approximate value of the wavelength for different Froude numbers, one can conclude that we have long waves ($\Delta h << \lambda$), which is typical for fluid flows in shallow water (Ferreira, 2013; Fiorot *et al.*, 2015).

We also tried to evaluate another parameter of interest, which was the wave amplitude, that is, how its spatial evolution occurs, that is, we tried to evaluate its behavior after each record obtained by the sensors in different positions of the channel, and can be seen in Fig. 9.

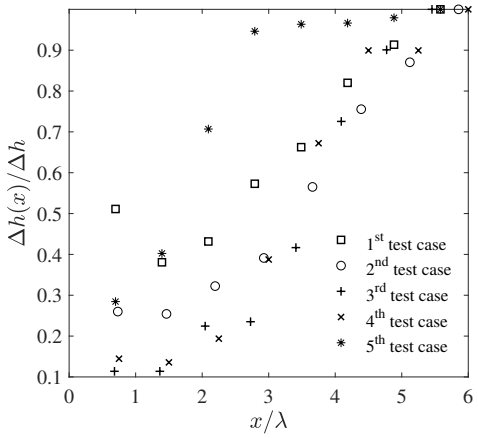


(a) Spatial evolution of roll waves.

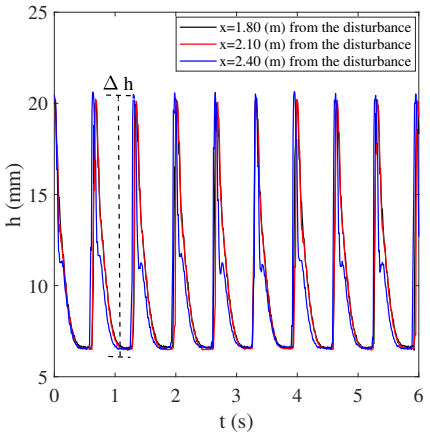


(b) Waveforms for the fifth test on three sensors $x = 1.8$, $x = 2.1$ and $x = 2.4$ m.

Figure 9: Spatial evolution of roll waves. For each simulation, roll waves spatial evolution follows the same behavior, and seem to stabilize after some wavelengths.

From Fig. 9 it is possible to see that the change in the volumetric flow rate and channel inclination implies directly the measurements of the wave amplitude. And yet, according to the Tab. 1 this fact also occurs with respect to the increase in the Froude number, which proves that the higher the Froude number, the greater should be the amplitude of the waves, this observation was also made by Ferreira (2013); Maciel *et al.* (2017).

Still, regarding the amplitude of the roll waves it can be said that they are very well defined, for example, see Fig. 9(b). When looking at each signal recorded by the sensor it can be seen that there is a small difference in amplitude when comparing them in the different positions of the sensors. However, it is considered that this discrepancy is related to the uncertainties of the measurement instruments (see Tab. 2). Furthermore, after a certain length of channel traveled they are in a stable regime. In addition, it is also considered that if we had an even longer channel it would be possible to perceive with greater precision the necessary distance that the roll wave must travel until the amplitude difference is not affected by the accuracy of the equipment.

## 4. CONCLUSION

In this paper the roll waves phenomenon was studied experimentally; these waves were generated in the laboratory by means of an experimental apparatus (a 3 m long channel). This instrument has made it possible to perform different tests in various scenarios (inclination and flow) with non-Newtonian fluid. The experimental apparatus has proven to be an efficient tool in reproducing pulsed waves under controlled conditions by means of a disturbance applied to the flow in which the waves were amplified to the point of reaching a stable shape propagating as a train of waves.

From the extracted results it was possible to explore dimensionless of interest, such as Reynolds and Froude, and also some properties of the flow and waves. From the device characterization tests it was possible to observe that deviations in the measurements no greater than 5% are visualized with respect to the flow rate measurements (consequently, F, R, $u_0$, etc.).

It was also possible to observe the spatio-temporal evolution of the roll waves and determine a dominant frequency from the obtained signal, and this is of the order of 1.5 Hz for both tests performed and measured in the different positions of the channel (Fig. 7). The same frequency is applied to the flow.

With respect to the measurement of roll waves, it was noted that the ultrasonic system performed well, measuring waves with steep fronts, amplitude, and well-defined period. In addition, it was observed that the waves needed to travel a certain length of the channel until they stabilized.

Finally, this type of work comes to contribute with others already existing in the literature in terms of experimental results of the phenomenon.

## 5. ACKNOWLEDGEMENTS

The author of this paper thanks the Sombrio Advanced Campus of the Catarinense Federal Institute for granting a full time leave for doctoral studies, via notice No. 21/2019.

## 6. REFERENCES

Aktershev, S. and Alekseenko, S., 2013. "Nonlinear waves and heat transfer in a falling film of condensate". *Physics of Fluids*, Vol. 25.

Balmforth, N.J. and Liu, J.J., 2004. "Roll waves in mud". *Journal of Fluid Mechanics*, Vol. 519, p. 33–54.

Balmforth, N., Bush, J. and Craster, R., 2005. "Roll waves on flowing cornstarch suspensions". *Physics Letters A*, Vol. 338, No. 6, pp. 479–484. ISSN 0375-9601.

Brock, R.R., 1969. "Development of roll waves in open channels." *Journal Hydraulics Division*, Vol. 95, pp. 1401–1427.

Coussot, P., 1994. "Steady, laminar, flow of concentrated mud suspensions in open channel". *Journal of Hydraulic Research - J HYDRAUL RES*, Vol. 32, pp. 535–559.

Cunha, E.F., 2018. *Implementação de um aparato experimental para medição de instabilidade em superfície livre com fluido não newtoniano.* Doutorado em Engenharia mecânica, Universidade Estadual Paulista - UNESP, Ilha Solteira/SP.

D'Alessio, S.J.D. and Pascal, J.P., 2008. "A mathematical and numerical study of roll waves". *WIT Transactions on Engineering Sciences*, Vol. 59, pp. 1–10.

Di Cristo, C., Iervolino, M. and Vacca, A., 2013. "On the applicability of minimum channel length criterion for roll-waves in mud-flows". *Journal of Hydrology and Hydromechanics*, Vol. 61, No. 4, pp. 286–292.

Ferreira, F.O., 2013. *Estabilidade e controle dinâmico de roll waves.* Doutorado em Engenharia Elétrica, Universidade Estadual Paulista - UNESP, Ilha Solteira/SP.

Ferreira, F.O., Maciel, G.F. and Pereira, J.B., 2021. "Roll waves and their generation criteria". *Brazilian Journal of Water Resources*, Vol. 26. ISSN 2318-0331.

Fiorot, G.H., 2012. *Mitigação de riscos e catástrofes naturais: análise numérico-experimental de roll waves evoluindo em canais inclinados.* Mestrado em Engenharia Mecânica, Universidade Estadual Paulista - UNESP, Ilha Solteira/SP.

Fiorot, G., Maciel, G., Cunha, E. and Kitano, C., 2015. "Experimental setup for measuring roll waves on laminar open channel flows." *Flow Measurement and Instrumentation.*, Vol. 41, pp. 149 – 157.

Maciel, G.F., Toniati, A.L. and Ferreira, F.O., 2021. "Cultura de gestão de riscos na mitigação de desastres naturais." *Revista Ibero Americana de Ciências Ambientais.*, Vol. 12, No. 2, pp. 671–686.

Maciel, G., Ferreira, F. and Fiorot, G., 2013. "Control of instabilities in non-newtonian free surface fluid flows". *Journal of the Brazilian Society of Mechanical Sciences and Engineering*.

Maciel, G., Ferreira, F., Cunha, E. and Fiorot, G., 2017. "Experimental apparatus for roll-wave measurements and comparison with a 1d mathematical model". *Journal of Hydraulic Engineering*, Vol. 143, No. 11, p. 04017046.

Minussi, R. and Maciel, G., 2012. "Numerical experimental comparison of dam break flows with non-newtonian fluids. j braz soc mech sci eng xxxiv(2):167-178". *Journal of the Brazilian Society of Mechanical Sciences and Engineering*, Vol. 34, pp. 167–178.

Needham, D.J. and Merkin, H., 1984. "On roll waves down an open inclined channel". *Journal Mathematical Physical & Engineering Sciences*, Vol. 394, pp. 259–278.

Ng, C.O. and Mei, C.C., 1994. "Roll waves on a shallow layer of mud modelled as a power-law fluid". *Journal of Fluid Mechanics*, Vol. 263, p. 151–184.

Noble, P., 2007. "Linear stability of viscous roll waves". *Communications in Partial Differential Equations - COMMUN PART DIFF EQUAT*, Vol. 32, pp. 1681–1713.

Piau, J., 2007. "Carbopol gels: Elastoviscoplastic and slippery glasses made of individual swollen sponges: Meso- and macroscopic properties, constitutive equations and scaling laws". *Journal of Non-Newtonian Fluid Mechanics*, Vol. 144, No. 1, pp. 1–29. ISSN 0377-0257.

Rocho, V.R., Fiorot, G.H. and Möller, S.V., 2020. "Linear Stability Analysis of Non-Newtonian Free Surface Flows a Mathematical Study on the Temporal and Spatial Branches." In *Annals of the 18th Brazilian Congress of Thermal Sciences and Engineering*. doi:https://abcm.org.br/proceedings/view/CIT20/0197.

## 7. RESPONSIBILITY NOTICE

The authors are solely responsible for the printed material included in this paper.